Wind Intensity Is Key to Phytoplankton Spring Bloom Under Climate Change

Frode B. Vikebø[1,2]*, Kjersti Opstad Strand[2,3] and Svein Sundby[3]

[1] Marine Processes and Human Impacts, Institute of Marine Research, Bergen, Norway, [2] Bjerknes Centre for Climate Research, University of Bergen, Bergen, Norway, [3] Section for Oceanography and Climate, Institute of Marine Research, Bergen, Norway

The onset of the spring bloom (OSB) occurs when phytoplankton growth exceeds losses and is promoted by a transition from deep convection to a shallow mixing layer concurrent with increasing light intensities in nutrient-enriched waters. We have combined remotely sensed chlorophyll-a data and high-resolution sea-surface winds to quantify and understand high-latitude spring-bloom dynamics and the effect of varying winds. Increasing winds strengthen turbulent mixing and may eventually cause the mixing depth to extend beyond the depth at which light is favorable for net growth and delay the OSB. We find that wind intensity accounts for up to 60% of the interannual variation in the OSB as revealed by remotely sensed chlorophyll-a values at the key spawning ground (62–63°N) of one of the worlds' largest herring stocks. The OSB is, on average, 1 month later and with about half the variability farther north at the main spawning ground (67–68°N) of one of the world's largest cod stocks. Since the atmospheric reanalysis considered here extends wind time series much further back in time (1958) than remote sensing (1998), the former may act as a good proxy for investigating OSB trends on the time scales of multi-decadal variability and climate change. We find a weak but non-significant signal of delay in the OSB across these extended time periods. More importantly, our results clearly show that predictions of future productivity and ecosystem dynamics under global warming based on earth system models require accurate representation of winds.
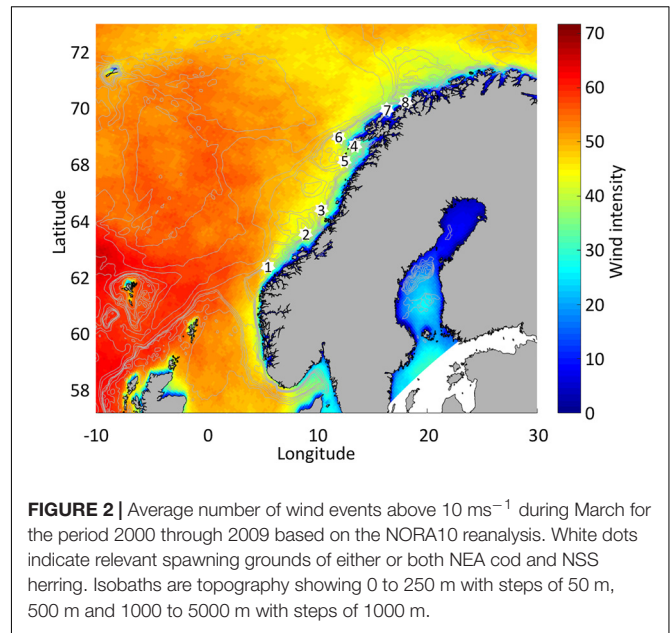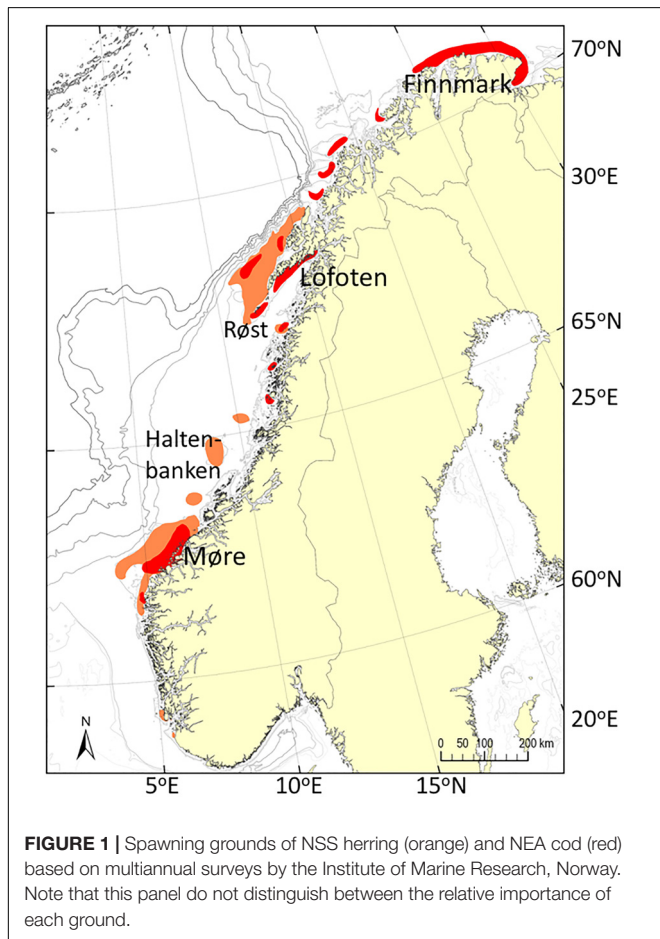
Keywords: SeaWiFS, MODIS, remote sensing, chlorophyll-a, fish larvae

INTRODUCTION

Timing of fish spawning to match the onset of the spring bloom (OSB), that in turn triggers the egg production of the herbivorous *Calanus finmarchicus* (Melle and Skjoldal, 1998; Kaartvedt, 2000), is a key to secure sufficient and suitable prey for the larval fish (Ellertsen et al., 1989). The Norwegian shelf is a typical spring-bloom system with an abrupt and limited duration of phytoplankton production during spring (Sundby et al., 2016) that is delayed with increasing latitudes (Vikebø et al., 2012). A multitude of processes and mechanisms jointly affect phytoplankton dynamics at high latitudes both during spring bloom and throughout the year as summarized by Lindemann and St. John (2014) and Chiswell et al. (2015). Concerning the spring bloom, Lindemann and St. John (2014) refer to the *Convection-Shutdown-Hypothesis* (Ferrari et al., 2014) arguing that spring bloom occurs when seasonal heating shuts down deep convection and vertical mixing is in accordance

with *Critical Turbulence* (Huisman et al., 1999). That is, weak enough to stratify phytoplankton in a density-unstratified water column. At very high latitudes, particularly north of the Arctic Circle, it has been suggested that the extreme seasonal light cycle has a more dominant influence than other factors on OSB through photoperiodic control of spore formation (Eilertsen et al., 1995).

The Norwegian Spring Spawning (NSS) herring (*Clupea harengus*) and the Northeast Arctic (NEA) cod (*Gadus morhua*) represent key pelagic and demersal species, respectively, and are among the world's largest herring and cod stocks. They both spawn patchwise during March to April at the Norwegian continental shelf north of 62°N (Olsen et al., 2010; Ottersen et al., 2014; **Figure 1**). The NSS herring spawns between Møre (62°N) and Vesterålen (69°N) with the main spawning area during recent years at the Møre Banks (62–63°N) (location 1 in **Figure 2**). NEA cod spawns between Møre and Finnmark (71°N) with the main spawning area in Lofoten (68°N) (Sundby and Nakken, 2008) (location 1–8 in **Figure 2**). The newly hatched larvae of both species drift pelagically northeastward along the coast and into the Barents Sea. They absorb their yolk-sac within days (5–7 days for NEA cod), after which they are entirely dependent on exogenous food (Folkvord, 2005). Naupliar and subsequently copepodite stages of spring-spawning

FIGURE 2 | Average number of wind events above 10 ms^{-1} during March for the period 2000 through 2009 based on the NORA10 reanalysis. White dots indicate relevant spawning grounds of either or both NEA cod and NSS herring. Isobaths are topography showing 0 to 250 m with steps of 50 m, 500 m and 1000 to 5000 m with steps of 1000 m.

copepods, particularly *C. finmarchicus*, are key prey items for fish early-life stages (ELS) of the NEA cod (Sysoeva and Degtereva, 1965; Ellertsen et al., 1984) and the NSS herring (Dalpadado et al., 2000).

The time of peak spawning of NEA cod on decadal time scales is nearly constant and occurs annually around the first days of April (Ellertsen et al., 1989). Older and larger cod have a longer batch-spawning period (Kjesbu et al., 1996) but size-selective fisheries have resulted in the population now consisting of younger and smaller fish (Pedersen, 1984), though this trend appears to reverse recently. Hence, on multi-decadal time scales the time of spawning varies. In contrast, the peak spawning in NSS herring varies between years by up to a month (Husebø et al., 2009). While the seasonal change in light is fixed between years (although modified by clouds and shadowing through the water column for various reasons), the seasonal shutdown of deep mixing with subsequent stabilization of the water column and the depth of the mixing layer are more variable.

Platt et al. (2003) showed that most of the variability in haddock larval survival off Nova Scotia (89%) could be accounted for by changes in timing of the phytoplankton bloom as deduced from remote sensing chlorophyll-a. Similar predictive strength was found for the temperate fish species rainbow wrasse (*Coris julis*) off the Azores (Fontes et al., 2016). However, caution is needed when considering environment-recruitment correlations as they seldom hold when extending the original time series (Myers, 1998). Also, remote sensing data only capture the surface manifestation of the bloom and may therefore not necessarily represent a larger part of the water column.

In situ measurements of the spring bloom along with other concurrent oceanic and atmospheric data have been collected at various locations to examine the main mechanisms whereby the timing of the bloom may shift. Collins et al. (2009) found that winds were the main regulator of the OSB in the Strait of Georgia

FIGURE 1 | Spawning grounds of NSS herring (orange) and NEA cod (red) based on multiannual surveys by the Institute of Marine Research, Norway. Note that this panel do not distinguish between the relative importance of each ground.

with strong winds deepening the mixed layer and delaying the bloom. In contrast, Mignot et al. (2016) found that the OSB in the Norwegian Sea was mainly determined by the photoperiod, starting as soon as light levels exceeded a fixed threshold. Indeed, Braarud et al. (1958) found a 2–3 weeks delay in OSB from Møre (62°N) to Lofoten-Vesterålen (69°N), but Rey (1981) showed that this delay also varied among years. At the shelf, near freshwater sources, the OSB may occur early if nutrients are added through elevated freshwater runoff but also delayed if strong wind events occur (Yin et al., 1996). Hence, episodes of strong wind can delay the necessary structuring of the water column and thereby disrupt favorable bloom conditions in various ways as reviewed by Lindemann and St. John (2014) with a delay of blooming as a consequence.

Herein, we focus on one important forcing relevant to the timing of spring bloom by comparing wind reanalysis covering the period 1958–2017 and a compilation of SeaWiFS and MODIS remote-sensed Chl-a for the period 1998–2017. The remote sensing data are compared to events of strong winds during the initiation of spring bloom. We hypothesize that there is a positive relationship between wind intensity and a delay in the OSB. In particular, we address the following questions; (i) when does OSB occur along the coast and how does it differ between shallow and deeper parts of the shelf, (ii) how does it vary between years, (iii) does this variation compare to concurrent variation in the number of strong wind events, and (iv) are there trends in the number of strong wind events across the extended period dating back to 1958.

DATA AND METHODS

SeaWiFS and MODIS Data

The SeaWiFS data are collected by NASA, processed and disseminated for use at https://oceandata.sci.gsfc.nasa.gov/SeaWiFS/Mapped/8-Day/9km/chlor_a/. The O'Reilly band ratio OCx and Hu color index algorithms are applied to obtain Chl-a, after which data are binned onto global maps (O'Reilly et al., 1998). We have downloaded 8-day composites (to allow for cloud variability) on a 9 by 9 km horizontal resolution covering the period 1998–2008. The MODIS (aqua) data were also collected by NASA, processed and disseminated for use at https://oceandata.sci.gsfc.nasa.gov/MODIS-Aqua/Mapped/8-Day/9km/chlor_a/ (O'Reilly et al., 2000). Again, we used the 8-day composites and 9 by 9 km horizontal resolution data covering the period 2003 to 2017. Previous studies have addressed the consistency of the time series for SeaWiFS and MODIS data and found that they are comparable and therefore suitable to combine (Zhang et al., 2006).

It was necessary to group bins both temporally and spatially to obtain sufficient data to quantify the OSB on the continental shelf, here defined to be shallower than 500 m. The OSB was selected to be when Chl-a rose above a threshold level and persisted for at least two consecutive 8-day composites. The threshold level used here (0.85 mg Chl-a m^{-3}) is the median of all Chl-a values in waters shallower than 300 m between 60.0 and 70.5°N for the combined SeaWiFS and

MODIS data in the period 1998 to 2017. This threshold is similar to the 1.0 mg Chl-a m^{-2} used in Stenevik et al. (2007), 5% above the annual median in Henson et al. (2009) and the 0.93 mg Chl-a m^{-2} in Vikebø et al. (2012). The OSB was resolved in 1.5 degree latitudinal bins between 60.0 and 70.5°N, distinguishing between data in waters deeper and shallower than 300 m. We chose 300 m as the inner and main branch of the strongly topographically steered the Norwegian Coastal Current (NCC) flows along isobaths on the shallower side of this separation line. We also quantified the corresponding standard deviation (std, std.m in matlab) of interannual variability in OSB.

NORA10 Reanalysis

Winds were taken from a dynamic downscaling of the ERA40 reanalysis (Uppala et al., 2005) at 10 m over a 10 by 10 km horizontal grid covering the Nordic Seas and the Barents Sea entitled NORA10 (Reistad et al., 2011). NORA10 covers the period 1958–2017 and provided 6-h values of winds. Comparison against in-situ observations reveals significant improvements as compared to ERA-40, but errors still remain, e.g., NORA10 winds are biased low for the highest wind speeds near the coast.

To compare winds with OSB, we compiled time series of annual number of 6-h winds above 10 ms^{-1} for the month of March. The threshold of 10 ms^{-1} was chosen as it represents a wind strength that significantly affects stratification in the water column (Strand et al., 2018). Note that we have not posed a requirement of persistence in winds to last for repeated 6-h wind sequences. We tested the sensitivity of the results to the threshold assumption. The month of March was chosen because it is the period immediately prior to the OSB at these latitudes (Vikebø et al., 2012). However, the OSB does occur later with increasing latitudes and the delay between Møre (approximately 62.5°N) and Lofoten (approximately 68.0°N) is reported to be about 35 days (Vikebø et al., 2012).

Data Analysis

Correlation analysis (corrcoef.m in matlab giving Pearson correlation) was carried out at every grid cell of the NORA10 grid between the number of wind events above the chosen threshold and the corresponding latitudinally binned OSB derived from remotely sensed Chl-a. In addition, we have quantified the correlation between wind events and OSB at well-known spawning grounds (SGs) of NEA cod and NSS herring (**Figure 2**). Mature NEA cod migrate from over-wintering areas in the Barents Sea to either of the multiple SGs along the Norwegian coast. They spawn in the transition layer between deeper Atlantic Water and Coastal Water above during March through April with peak spawning in early April (Ellertsen et al., 1989). The main SGs are both inside and outside the Vestfjord in Lofoten, though SGs also include locations farther south and north (Sundby and Nakken, 2008). Mature NSS herring over-winter currently on the shelf and in fjords to the north of Lofoten and thereafter migrate to SGs mainly at Møre, but also partly near Haltenbanken and south of the island Røst (Olsen et al., 2010). **Figure 2** shows important SGs for both NEA cod and NSS herring.

RESULTS

Wind Events Above 10 ms^{-1} in March

During the years 2000–2009 the number of events where 6-h winds during March exceeded 10 ms^{-1} was particularly high in an area tangent to the Norwegian coast from west-southwest before diverging north-northeast at an increasing distance from the coast (**Figure 2**). Hence, the number of high wind episodes is higher close to the mid-Norwegian coast (62°N) than farther north. Northwards along the coast from 62°N the number of events drops from more than 40–50 to less than 30–40.

Onset of Spring Bloom

The mean OSB from 1998 to 2017 was delayed with increasing latitudes from 8 to 14 March between 60.0 to 63.0°N including Møre, to 12–14 April between 66.0 to 69.0°N including Lofoten (**Table 1**). In general, there is less variability in OSB in the Lofoten than farther south and north, with about 68% of the data (1 std.) within ± 7 days. Farther off the coast in deeper waters the OSB is generally later in the year and most often with a higher degree of inter-annual variability.

Concurrent High Wind Events and Delay in Spring Bloom

Similar patterns emerge when comparing time series of the number of 6-h wind events during March for the period 1998 to 2017 with the time of OSB as inferred from remote sensing data based on the combined SeaWiFS and MODIS (**Figure 3**). Strong correlations are found at the shelf off Møre between 62.5 and 64.5°N (correlation coefficient R^2 between 0.35 and 0.60 with significance $P < 0.01$), while weaker but still significant (well

within the 10% percentile) correlation is found in the region stretching from about 64.5 to 66.0°N (R^2 between 0.25 and 0.35). Even farther north, in the region stretching from 66.0 to about 67.5°N and 69 to 70°N, the correlation is often still significant but weak (R^2 between 0.1 and 0.2).
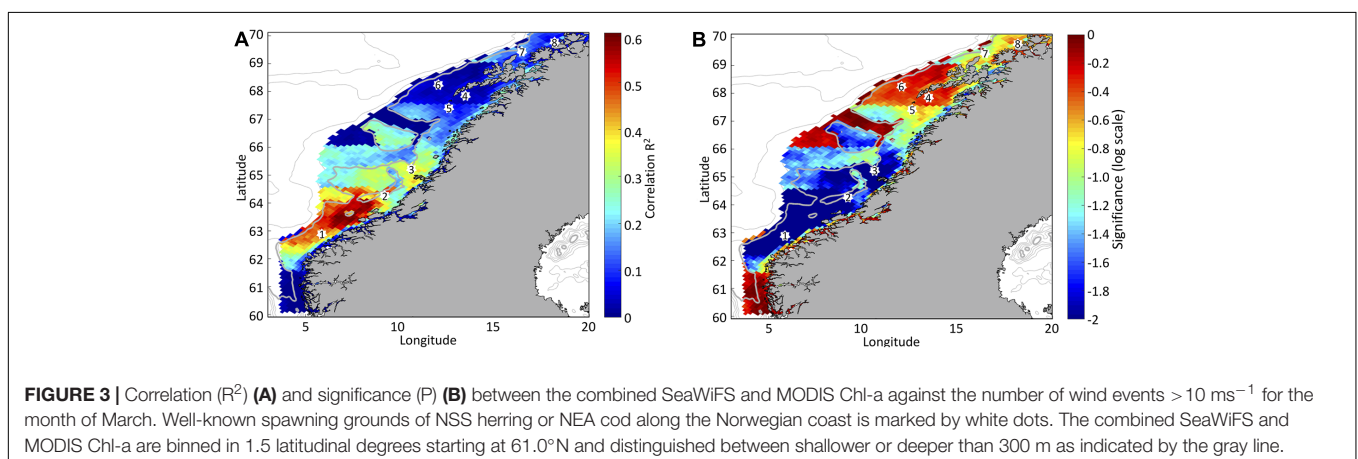
In general, deeper parts of the shelf, such as the trough penetrating the continental shelf at about 67°N, have weaker correlations between strong wind events and OSB. Also, the ability of wind events to predict OSB is particularly low in Lofoten, between 67.5 and 69°N, a very dynamic region of the shelf where the two branches of the NCC and the Norwegian Atlantic Slope Current meet.
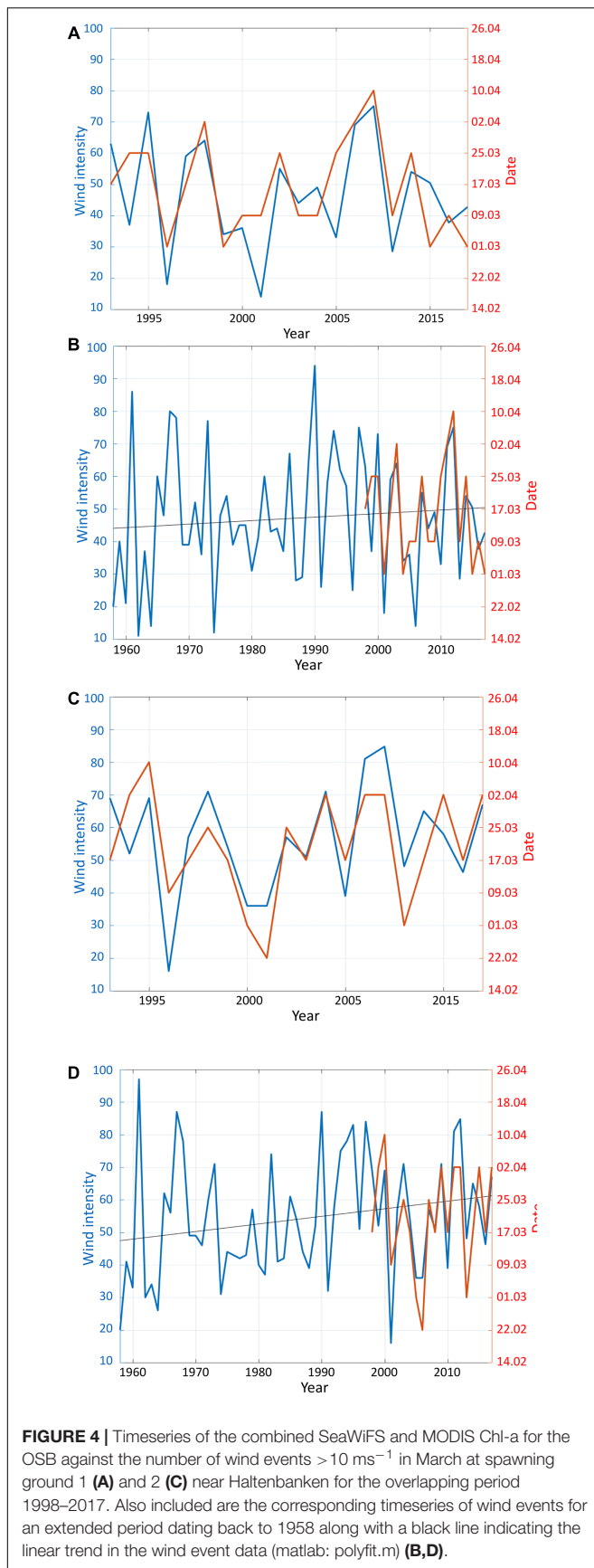
Winds and Spring Bloom at NEA Cod and NSS Herring Spawning Grounds

The number of events where March 6-h winds rise above 10 ms^{-1} together with year-specific OSB from remote sensing at well-known SGs of NEA cod and NSS herring (**Figures 4A,C**) reflect the patterns described above. **Table 2** shows that at the main SG of NSS herring at Møre (SG1), the number of wind events above 10 ms^{-1} accounts for 45.2% of the variability in OSB. Farther north, around Haltenbanken (SG2) at about 64.5°N, the explanatory capability of winds is even higher, reaching 50.4%. However, around Lofoten and the adjacent region to the north, the concurrent interannual variations in the two variables show low co-variation, though south of Røst (SG5) the wind events still account for 12.5% of the interannual variation in OSB with $P < 0.13$. North of Lofoten (SG7 and 8), as the flow is dominated by a single NCC branch and the shelf is extraordinary narrow, the explanatory capability of wind events in March on the OSB again rises but not to the levels observed at Møre.

TABLE 1 | Average day of OSB with standard deviation for waters in 1.5 degree latitudinal intervals between 60.0 and 70.5°N for waters shallower (A) and deeper (B) than 300 m (OSBs are in dates in the format dd.mm, while standard deviation Std is in number of days).

Lat (°N)	60.0–61.5	61.5–63.0	63.0–64.5	64.5–66.0	66.0–67.5	67.5–69.0	69.0–70.5
OSB A	08.03	14.03	23.03	14.04	14.04	12.04	29.04
Std A	12.0	12.1	15.4	9.7	5.7	7.0	19.7
OSB B	20.03	05.04	11.04	17.04	29.04	19.04	15.04
Std B	14.3	12.3	12.8	11.3	12.9	10.9	12.1

FIGURE 3 | Correlation (R^2) **(A)** and significance (P) **(B)** between the combined SeaWiFS and MODIS Chl-a against the number of wind events >10 ms^{-1} for the month of March. Well-known spawning grounds of NSS herring or NEA cod along the Norwegian coast is marked by white dots. The combined SeaWiFS and MODIS Chl-a are binned in 1.5 latitudinal degrees starting at 61.0°N and distinguished between shallower or deeper than 300 m as indicated by the gray line.

FIGURE 4 | Timeseries of the combined SeaWiFS and MODIS Chl-a for the OSB against the number of wind events >10 ms^{-1} in March at spawning ground 1 **(A)** and 2 **(C)** near Haltenbanken for the overlapping period 1998–2017. Also included are the corresponding timeseries of wind events for an extended period dating back to 1958 along with a black line indicating the linear trend in the wind event data (matlab: polyfit.m) **(B,D)**.

While the remote sensing data from the combined SeaWiFS and MODIS only date back to 1998, the NORA10 archive goes back to 1958. Hence, in areas with strong correlation between winds and OSB during the time of overlapping time series, winds may act as a proxy for OSB at times prior to the remote sensing data. At the southernmost SGs, NORA10 shows that previous times had higher variability than during the overlap with the remote sensing data (**Figures 4B,D**). Also, there were generally more frequent strong winds during the 1990s and less so during the 1970s and 1980s.

By fitting linear curves to the time series of wind events above 10 ms^{-1} (polyfit.m in matlab) for the month of March (**Figures 4B,D**), it becomes clear that at all SGs investigated there is a general positive trend toward more frequent strong winds, indicating a delay in OSB (**Table 3**). However, the positive trends are all weak except for SG2 and 3 where the trends account for 4.9 and 4.1% of the variability with P at 0.09 and 0.12, respectively.

Sensitivity to Wind Threshold and Period

We have rerun our calculations using (i) a threshold for winds of 7 instead of 10 ms^{-1} and (ii) extracted a 1-month long count of wind events above the threshold according to the average latitudinal time of OSB. More specifically, we have extracted winds during 20 days before and 10 days after the latitudinal bin-specific average time of OSB, motivated by our expectations that winds on average do delay OSB along the coast. Based on **Table 1**, this corresponds to extracting winds during March only for the latitudinal bin 63.0–64.5°N while the bins to the south and north are earlier or later, respectively. Though not shown here, no combinations of thresholds or alternative periods of extracting winds improve the correlation between winds and OSB as compared to our initial selection of criteria.

DISCUSSION

High-latitude ecosystems are dominated by a strong seasonal variation in primary productivity with a peak during spring and with a limited duration that sets the scene for the regional trophodynamics (Sundby et al., 2016). The increasing influence of the seasonality in light with higher latitudes, particularly north of the Arctic Circle, is reflected in short and intense spawning periods at higher trophic levels. According to Sverdrup's (1953) Critical-Depth-Hypothesis the main forces that regulate the spring bloom are the vertical flux of nutrients from the ocean deep to the upper layer during winter mixing, the increase of light after winter darkness and the subsequent stabilization of the water column with seasonal heating and freshwater melting. This causes the mixed-layer depth to become shallower than the critical depth allowing phytoplankton production to start. Sverdrup's original theory has, however, been modified by subsequent authors as reviewed by Lindemann and St. John (2014), acknowledging additional processes and mechanisms that act in concert to shape the spring bloom. These include among others that (i) the mixing layer may be shallower than the mixed layer allowing early onset of spring bloom before the water column becomes stratified, (ii) phytoplankton net growth

TABLE 2 | Correlation (R^2) and significance (P) between the combined SeaWiFS and MODIS Chl-a against the number of wind events >10 ms^{-1} in March at 8 well-known spawning grounds of NSS herring or NEA cod along the Norwegian coast.

SG	1	2	3	4	5	6	7	8
R^2	0.4524	0.5035	0.3792	0.0424	0.1249	0.0331	0.2131	0.1887
P	0.0012	0.0005	0.0038	0.3837	0.1264	0.4429	0.0538	0.0717

TABLE 3 | Correlation (R^2) and significance (P) between time against the number of wind events >10 ms^{-1} in March at 8 well-known spawning grounds of NSS herring or NEA cod along the Norwegian coast.

SG	1	2	3	4	5	6	7	8
R^2	0.0091	0.0491	0.0410	0.0018	0.0225	0.0166	0.0054	0.0034
P	0.4676	0.0890	0.1207	0.7442	0.2529	0.3266	0.5780	0.6593

require a critical level of turbulent mixing with an upper and lower limit, (iii) the phytoplankton loss rate is highly variable due to, e.g., variable grazing, (iv) phytoplankton sinking rates are highly dependent on size and shape that vary with the ambient conditions. Nevertheless, though there are multiple processes affecting OSB, strong wind-induced mixing at high latitudes is detrimental for OSB. Moreover, OSB at very high latitudes, i.e., poleward of around the Arctic Circle, seems to be more controlled by the strong seasonal changes in photoperiod than in the mixing processes and the stratification, as shown by Eilertsen et al. (1995), possibly also due to the particular phytoplankton species composition at these latitudes (Degerlund and Eilertsen, 2010). Here, we have used remotely sensed Chl-a data to investigate spatiotemporal dynamics of the OSB along the Norwegian coast and how it may vary in response to winds. The winds affect the upper oceans through frictional stress that transfers energy to the ocean generating waves, currents and mixing. Hence, the wind stress increases the turbulent mixing in the mixing layer and deepens its base. Eventually, this may extend the upper mixing layer beyond the critical depth and delay the bloom onset.

We find our hypothesis that higher wind intensity delays the OSB to be statistically supported in part of the investigated domain, particularly within 62.5–64.5°N, which overlaps with the main SG of NSS herring (**Figure 3A**). On average, there is a delay in the OSB of 1 month between the main SGs of the NSS herring (Møre, 62–63°N) and the NEA cod (Lofoten, about 68°N) (**Table 1**). During this interval mean wind speed drops due to the shift from winter to summer conditions. Similarly, there is a delay of several weeks between the shallow regions close to the coast and the deeper parts toward the shelf edge. The interannual variation in OSB changes considerably along the coast, with the variability in Lofoten of about half that at Møre. Also, by using wind intensity as a proxy for the OSB, thereby enabling extrapolation back to 1958, we find a non-significant but positive trend corresponding to a delay in OSB (**Table 3**).

The area of higher predictive capacity of wind intensities for the OSB between 62.5 and 64.5°N is concurrent with areas where climatology indicates particularly frequent strong winds. Also, frequencies of strong winds decrease with time during spring, so that at higher latitudes, where OSB occurs later, the winds are generally less energetic (Dickson et al., 1988). The less variable

OSB with increasing latitude is not surprising given that the transition from winter dark to summer light becomes more rapid toward the north.

The delay in OSB away from the coast as derived from remote sensing is consistent with Blindheim (1989) and Pavshtiks and Timokhina (1972). A possible mechanism is that while stratification off the coast is caused by thermal insulation through seasonal heating, the stratification along the coast is also facilitated by salinity stratification which, to a variable degree, exists throughout winter. We know from earlier studies (e.g., Vikebø et al., 2010) and drifter studies (Saetre, 2007) that larval fish from the Møre spawning areas may drift either close to the coast or along the shelf edge because of the two branches in the NCC. Clearly, remotely sensed Chl-a indicates that larvae following the NCC branch close to the shelf edge are offered less food than conspecifics closer to the coast if they are spawned early in the season.

An additional factor that may further amplify the delay in bloom onset is that strong winds associated with low pressures in the northeastern part of the North Atlantic are, in general, co-occurring with higher cloud cover (Previdi and Veron, 2007). This may in turn reduce the penetration of short-wave radiation necessary for the photosynthetic activity in the photic zone (Platt and Sathyendranath, 1988). Hence, under such conditions, the depth of the critical layer might shallow owing to reduced light intensity while at the same time the base of the mixing layer deepens due to increased wind.

It seems easier for spawning fish to match prey for their offspring in Lofoten than at Møre because of less interannual variation in the OSB dates, assuming larval fish prey production is triggered by the OSB. Sundby and Nakken (2008) showed that the NEA cod latitudinal spawning distribution has varied on multi-decadal scales owing to similar scale variation in environmental temperatures. Opdal and Jørgensen (2015) suggested an alternative, but not contradictive, explanation involving size-selective fisheries. However, Langangen et al. (2019) supported the hypothesis of climate-driven shifts based on analysis of more recent data (2000–2016) during a recovery of cod stock demography. Contrary, there is no indication of temporally varying time of spawning. NEA cod spawn during the months of March and April with a peak in early April (Ellertsen et al., 1989). Hence, despite the OSB varies considerably while

the time of peak spawning does not, the NEA cod spawning occurs during an extended period not least due to multiple batch spawning so that at least some of its offspring match suitable prey concentrations. Hence, dependent on the OSB and the subsequent acceleration of zooplankton reproduction this may provide prey for many or few larvae. NSS herring on the other hand has a highly variable time of spawning and is negatively correlated with adult over-wintering temperature and positively correlated with the fraction of recruit spawners (Husebø et al., 2009). When at the same time there is large variation in OSB at the core spawning area of NSS herring, as predicted by remote-sensed Chl-a data, there is a higher chance of mismatch with prey as compared to NEA cod. This fits well with data showing that NSS herring is more robust to low food concentration than NEA cod (Folkvord et al., 2009, 2015).

With the potential relationship established between winds and OSB in parts of the investigated area, it is interesting to consider how this may develop under future climate change. Average winter storm track density based on NCEP-CFSRR reanalysis (Bader et al., 2011) determines where strong winds occur more frequently. According to these authors, there is disagreement among studies on whether extratropical cyclones in the North Atlantic have become stronger and/or more frequent. But they point to the study by Alexandersson et al. (1998) and Bärring and von Storch (2004) summarizing atmospheric pressure data across the Atlantic-European sector indicating a minimum around 1960, an increase to a maximum around 1990 and thereafter a decline toward 2000. Finally, they summarize that the majority of climate models indicate a poleward shift of northern hemisphere storm tracks in a future warmer climate, which likely will affect the OSB along the Norwegian coast. Under such a scenario the main NSS herring SG may experience less strong wind events. Currently, the dominating view is that a warming climate will result in an earlier and extended spring bloom because of a shallowing of the mixed layer and an earlier onset of favorable stratification for a bloom (Steinacher et al., 2010; Bopp et al., 2013). However, Kahru et al. (2010) show that high

latitudes (about 30–80°N), dominated by relatively strong winds as compared to low latitudes, experience decreased Chl-a during elevated winds. Oppositely, elevated winds at lower latitudes lead to increased Chl-a. This may be interpreted so that stronger winds at high latitudes where winds are already strong result in a deepening of a shallow mixing layer and a breakdown of stratification and the upper mixed layer. At low latitudes, stronger winds add to a relatively weaker wind field and contribute to replenishment of nutrients to the upper mixing layer. Hence, considering future productivity and ecosystem dynamics under global warming based on earth system models without having the winds correct may lead to erroneous predictions.

REFERENCES

Alexandersson, H., Schmith, T., Iden, K., and Tuomenvirta, H. (1998). Long-term variations of the storm climate over NW Europe. *Glob. Atmos. Ocean Syst.* 6, 97–120.

Bader, J., Mesquita, M. D. S., Hodges, I. H., Keelnyside, N., Østerhus, S., and Miles, M. (2011). A review on Northern Hemisphere sea-ice, storminess and the North Atlantic Oscillations: observations and projected changes. *Atmos. Res.* 101, 809–834. doi: 10.1016/j.atmosres.2011.04.007

Bärring, L., and von Storch, H. (2004). Scandinavian storminess since about 1800. *Geophys. Res. Lett.* 31:L20202. doi: 10.1029/2004GL020441

Blindheim, J. (1989). "Ecological features of the Norwegian Sea," in *Proceedings of the Sixth Conference of the Comité Arctique International*, eds Louis, R and V. Alexander (Leiden: E.J. Brill) 366–401.

Bopp, L., Resplandy, L., Orr, J. C., Doney, S. C., Dunne, J. P., Gehlen, M., et al. (2013). Multiple stressors of ocean ecosystems in the 21st century: projections with CMIP5 models. *Biogeosciences*, 10: 6225–6245. doi: 10.5194/bg-10-6225-2013

Braarud, T., Ringdal Gaarder, K., and Nordli, O. (1958). Seasonal changes in the phytoplankton at various points of the Norwegian west coast. *Fiskeridirektoratets Skrifter Serie Havundersøkelser* 12, 1–77.

Chiswell, S. M., Calil, P. H. R., and Boyd, P. W. (2015). Spring blooms and annual cycles of pkytoplankton: a unified perspective. *J. Plankton Res.* 37, 500–508. doi: 10.1093/plankt/jbv021

Collins, A. K., Allen, S. E., and Pawlowicz, R. (2009). The role of wind determining the timing of the spring bloom in the Strait of Georgia. *Can. J. Fish. Aquat. Sci.* 66, 1597–1616. doi: 10.1139/F09-071

Dalpadado, P., Ellertsen, B., Melle, W., and Dommasnes, A. (2000). Food and feeding conditions of Norwegian spring pawning herring (Clupea harengus) through its feeding migration. *ICES J. Mar. Sci.* 57, 843–857. doi: 10.1006/jmsc.2000.0573

Degerlund, M., and Eilertsen, H. C. (2010). Main species characteristics of phytoplankton spring blooms in NE atlantic and arctic waters (68-80 oN). *Estuaries Coast.* 33, 242–269. doi: 10.1007/s12237-009-9167-7

Dickson, R. R., Kelly, P. M., Colebrook, J. M., Wooster, W. S., and Cushing, D. H. (1988). North winds and production in the eastern North Atlantic. *J. Plankton Res.* 10, 151–169. doi: 10.1093/plankt/10.1.151

Eilertsen, H. C., Sandberg, S., and Tøllefsen, H. (1995). Photoperiodic control of diatom spore growth: a theory to explain the onset of phytoplankton blooms. *Mar. Ecol. Progr. Ser.* 116, 303–307. doi: 10.3354/meps116303

Ellertsen, B., Fossum, P., Solemdal, P., and Sundby, S. (1989). Relations between temperature and survival of eggs and first feeding larvae of the North-East

Arctic cod (Gadus morhua L.). *Rapports et procès verbaux des reunions, Conseil International pour l'Éxploration de la Mer* 191, 209–219.

Ellertsen, B., Fossum, P., Solemdal, P., Sundby, S., and Tilseth, S. (1984). "A case study on the distribution of cod larvae and availability of prey organisms in relation to physical processes in Lofoten," in *The Propagation of Cod, Gadus morhua L*, eds E. Dahl, D. S. Danielssen, E. Moksness, P. Solemdal (Arendal: Institute of Marine Research, Flødevigen Research Station), 453–478.

Ferrari, R., Merrifield, S. T., and Taylor, J. R. (2014). Shutdown of convection triggers increase of surface chlorophyll. *J. Mar. Syst.* 147, 116–122. doi: 10.1016/j.jmarsys.2014.02.009

Folkvord, A. (2005). Comparison of size-at-age of larval Atlantic cod (Gadus morhua) from different populations based on size- and temperature-dependent growth models. *Can. J. Fish. Aquat. Sci.* 62, 1037–1052. doi: 10.1139/f05-008

Folkvord, A., Fiksen, Ø., Høie, H., Johannesen, A., Otterlei, E., and Vollset, K. W. (2009). What can size distributions within cohorts tell us about ecological processes in fish larvae? *Sci. Mar.* 73, 119–130. doi: 10.3989/scimar.2009.73s1119

Folkvord, A., Vollset, K. W., and Catalan, I. A. (2015). Differences in growth and survival between cod Gadus morhua and herring Clupea harengus early stages co-reared at variable prey considerations. *J. Fish Biol.* 87, 1176–1190. doi: 10.1111/jfb.12783

Fontes, J., Semmens, B., Caselle, J. E., Santos, R. S., and Prakya, S. R. (2016). Ocean productivity may predict recruitment of the rainbow wrasse (Coris julis). *PLoS One* 11:e0165648. doi: 10.1371/journal.pone.0165648

Henson, S. A., Dunne, J. P., and Sarmiento, J. L. (2009). Decadal variability in North Atlantic phytoplankton blooms. *J. Geophys. Res.* 114:C04013. doi: 10.1029/2008JC005139

Huisman, J., van oostveen, P., and Weissing, F. J. (1999). Critical depth and critical turbulence: two different mechanisms for the development of phytoplankton blooms. *Limnol. Oceanogr.* 44, 1781–1787. doi: 10.4319/lo.1999.44.7.1781

Husebø, Å., Stenevik, E. K., Slotte, A., Fossum, P., Salthaug, A., Vikebø, F., et al. (2009). Effects of hatching time on year- class strength in Norwegian spring-spawning herring (Clupea harengus). *ICES J. Mar. Sci.* 66, 1710–1717. doi: 10.1093/icesjms/fsp150

Kaartvedt, S. (2000). Life history of *Calanus finmarchicus* in the Norwegian Sea in relation to planktivorous fish. *ICES J. Mar. Sci.* 57, 1819–1824. doi: 10.1006/jmsc.2000.0964

Kahru, M., Gille, S. T., Murtugudde, R., Strutton, P. G., Manzano-Sarabia, M., Wang, H., et al. (2010). Global correlations between winds and ocean chlorophyll. *J. Geophys. Res.* 115:C12040. doi: 10.1029/2010JC006500

Kjesbu, O. S., Solemdal, P., Bratland, P., and Fonn, M. (1996). Variation in annual egg production in individual captive Atlantic cod (Gadus morhua). *Can. J. Fish. Aquat. Sci.* 53, 610–620. doi: 10.1139/cjfas-53-3-610

Langangen, Ø., Färber, L., Stige, L. C., Diekert, F. K., Barth, J. M. I., Matschiner, M., et al. (2019). Ticket to spawn: combining economic and genetic data to evaluate the effect of climate and demographic structure on spawning distribution in Atlantic cod. *Glob. Change Biol.* 25, 134–143. doi: 10.1111/gcb.14474

Lindemann, C., and St. John, M. A. (2014). A seasonal diary of phytoplankton in the North Atlantic. *Front. Mar. Sci.* 1:37. doi: 10.3389/fmars.2014.00037

Melle, W., and Skjoldal, H. R. (1998). Reproduction and development of *Calanus finmarchicus*, C. Glacialis and C. hyperboreus in the Barents Sea. *Mar. Ecol. Progr. Ser.* 169, 211–228. doi: 10.3354/meps169211

Mignot, A., Ferrari, R., and Mork, K. A. (2016). Spring bloom onset in the Nordic Seas. *Biogeosciences* 13, 3485–3502. doi: 10.5194/bg-13-3485-2016

Myers, A. M. (1998). When do environment – recruitment correlations work? *Rev. Fish Biol. Fish.* 8, 285–305.

Olsen, E., Aanes, S., Mehl, S., Holst, J. C., Aglen, A., and Gjøsaeter, H. (2010). Cod, haddock, saithe, herring, and capelin in the Barents Sea and adjacent waters: a review of the biological value of the area. *ICES J. Mar. Sci.* 67, 87–101. doi: 10.1093/icesjms/fsp229

Opdal, A. F., and Jørgensen, C. (2015). Long-term change in a behavioural trait: truncated spawning distribution and demography in Northeast Arctic cod. *Glob. Change Biol.* 21, 1521–1530. doi: 10.1111/gcb.12773

O'Reilly, J. E., Maritorena, S., Mitchell, B. G., Siegel, D. G., Carder, K. L., Garver, S. A., et al. (1998). Ocean color chlorophyll algorithms for SeaWiFS. *J. Geophys. Res.* 103, 24937–24953. doi: 10.1029/98jc02160

O'Reilly, J. E., Maritorena, S., Siegel, D., O'Brien, M. C., Toole, D., Mitchell, B. G., et al. (2000). "Ocean color chlorophyll algorithms for SeaWiFS, OC2, and OC4: Version 4," in *SeaWiFS Postlaunch Technical Report series seawifs Postlaunch Calibration and Validation Analyses, Part 3*, eds S. B. Hooker, and E. R. Firestone (Greenbelt, MD: NASA Goddard Space Flight Center). doi: 10.1029/98jc02160

Ottersen, G., Bogstad, B., Yaragina, N. A., Stige, L. C., Vikebø, F. B., and Dalpadado, P. (2014). A review of early life history dynamics of Barents Sea cod (Gadus morhua). *ICES J. Mar. Sci.* 71, 2064–2087. doi: 10.1093/icesjms/fsu037

Pavshtiks, E. A., and Timokhina, A. F. (1972). History if investigations on plankton in the Norwegian sea and the main results of soviet investigations. *Proc. R. Soc. Edinburgh. Sect. B Biol.* 73, 267–278. doi: 10.1017/S0080455X00002320

Pedersen, T. (1984). "Variation of peak spawning of Arcto-Norwegian cod (Gadus morhua L.) during the time period 1929–1982 based on indices estimated from fishery statistics," in *The Propagation of Cod Gadus morhua L*, eds E. Dahl, D. S. Danielssen, E. Moksness, and P. Solemdal (Arendal: Institute of Marine Research, Flødevigen Research Station).

Platt, T., Fuentes-Yaco, C., and Frank, K. T. (2003). Spring algal bloom and larval fish survival. *Nature* 423, 398–399. doi: 10.1038/423398b

Platt, T., and Sathyendranath, S. (1988). Oceanic primary production: estimation by remote sensing at local and regional scales. *Science* 241, 1613–1620. doi: 10.1126/science.241.4873.1613

Previdi, M., and Veron, D. E. (2007). North Atlantic cloud cover response to the North Atlantic oscillation and relationship to surface temperature changes. *J. Geophys. Res.* 112:17. doi: 10.1029/2006JD007516

Reistad, M., Breivik, Ø., Haakenstad, H., Aarnes, O. J., Furevik, B. R., and Bidlot, J. R. (2011). A high-resolution hindcast of wind and waves for the North Sea, the Norwegian Sea, and the Barents Sea. *J. Geophys. Res.* 116:C05019. doi: 10.1029/2010JC006402

Rey, F. (1981). "The development of the spring phytoplankton outburst at selected sites off the Norwegian coast," in *Proceedings from the Norwegian Coastal Current Symposium*, R. Saetre, and M. Mork (Bergen: University of Bergen).

Saetre, R. (ed.) (2007). *The Norwegian Coastal. (current): Oceanography and Climate.* Trondheim: Tapir Academic Press.

Steinacher, M., Joos, F., Frölicher, T. L., Bopp, L., Cadule, P., Cocco, V., et al. (2010). Projected 21st century decrease in marine productivity: a multi-model analysis. *Biogeosciences* 7, 979–1005. doi: 10.5194/bg-7-979-2010

Stenevik, E. K., Melle, W., Gaard, E., Gislason, A., Broms, C. T. A., Prokopchuk, I., et al. (2007). Egg production of *Calanus finmarchicus* - a basin-scale study. *Deep Sea Res. II* 54, 2672–2685. doi: 10.1016/j.dsr2.2007.08.027

Strand, K. O., Vikebø, F. B., Sundby, S., Sperrevik, A. K., and Breivik, Ø. (2018). Subsurface maxima in buoyant fish eggs indicate vertical velocity shear and spatially limited spawning grounds. *Limnol. Oceanogr.* 64, 1239–1251. doi: 10.1002/lno.11109

Sundby, S., Kjesbu, O. S., and Drinkwater, K. (2016). The north atlantic spring-bloom system – where the changing climate meets the winter dark. *Front. Mar. Sci.* 3:28. doi: 10.3389/fmars.2016.00028

Sundby, S., and Nakken, O. (2008). Spatial shifts in spawning habitats of Arcto-Norwegian cod related to multidecadal climate oscillations and climate change. *ICES J. Mar. Sci.* 65, 953–962. doi: 10.1093/icesjms/fsn085

Sverdrup, H. U. (1953). On conditions for the vernal blooming of phytoplankton. *J. du Conseil Permanent International pour l'Exploration de la Mer* 18, 287–295. doi: 10.1093/icesjms/18.3.287

Sysoeva, T. K., and Degtereva, A. A. (1965). The relation between the feeding of cod larvae and pelagic fry and the distribution and abundance of their principal food organisms. *ICNAF Spec. Publ.* 6, 411–416.

Uppala, S. M., Kållberg, P. W., Simmons, A. J., Andrae, U., Costa Bechtold, V. D., Fiorino, M., et al. (2005). The ERA-40 re-analysis. *Q. J. R. Meteorol. Soc.* 131, 2961–3012.

Vikebø, F., Husebø, Å., Slotte, A., Stenevik, E. K., and Lien, V. (2010). Impact of hatching date, vertical distribution and interannual variation in physical forcing on northward displacement and temperature conditions of Norwegian spring-spawning herring larvae. *ICES J. Mar. Sci.* 67, 1948–1956. doi: 10.1093/icesjms/fsq084

Vikebø, F. B., Korosov, A., Stenevik, E. K., Husebø, Å., and Slotte, A. (2012). Spatio-temporal overlap of hatching in Norwegian spring- spawning herring and the

spring phytoplankton bloom at available spawning substrata. *ICES J. Mar. Sci.* 69, 1298–1302. doi: 10.1093/icesjms/fss083

Yin, K., Harrison, P. J., Goldblatt, R. H., and Beamish, R. J. (1996). Spring bloom in the central Strait og Georgia: interactions of river discharge, winds and grazing. *Mar. Ecol. Prog. Ser.* 138, 255–263. doi: 10.3354/meps13 8255

Zhang, C., Hu, C., Shang, S., Müller-Karger, F. E., Li, Y., Dai, M., et al. (2006). Bridging between SeaWiFS and MODIS for continuity of chlorophyll-a concentration assessments off Southeastern China. *Remote Sens. Environ.* 102, 250–263. doi: 10.1016/j.rse.2006.02.015